Building and Environment 245 (2023) 110893

Contents lists available at ScienceDirect

Building and Environment

journal homepage: www.elsevier.com/locate/buildenv

Data-driven control of airborne infection risk and energy use in buildings

Michael J. Risbeck [c,1], Alexander E. Cohen [a,1], Jonathan D. Douglas [c], Zhanhong Jiang [c], Carlo Fanone [d], Karen Bowes [d], Jim Doughty [e], Martin Turnbull [d], Louis DiBerardinis [e], Young M. Lee [c], Martin Z. Bazant [a,b,*]

[a] Department of Chemical Engineering, Massachusetts Institute of Technology, Cambridge, MA 02139, United States of America
[b] Department of Mathematics, Massachusetts Institute of Technology, Cambridge, MA 02139, United States of America
[c] Artificial Intelligence Group, Johnson Controls, Milwaukee, WI 53202, United States of America
[d] Department of Facilities, Engineering, and Energy Management, Massachusetts Institute of Technology, Cambridge, MA 02139, United States of America
[e] Environment, Health and Safety Office, Massachusetts Institute of Technology, Cambridge, MA 02139, United States of America

ARTICLE INFO

Keywords:
Airborne transmission
Indoor air quality
HVAC
Control

ABSTRACT

The global devastation of the COVID-19 pandemic has led to calls for a revolution in heating, ventilation, and air conditioning (HVAC) systems to improve indoor air quality (IAQ), due to the dominant role of airborne transmission in disease spread. While simple guidelines have recently been suggested to improve IAQ mainly by increasing ventilation and filtration, this goal must be achieved in an energy-efficient and economical manner and include all air cleaning mechanisms. Here, we develop a simple protocol to directly, quantitatively, and optimally control transmission risk while minimizing energy cost. We collect a large dataset of HVAC and IAQ measurements in buildings and show how models of infectious aerosol dynamics and HVAC operation can be combined with sensor data to predict transmission risk and energy consumption. Using this data, we also verify that a simple safety guideline is able to limit transmission risk in full data-driven simulations and thus may be used to guide public health policy. Our results provide a comprehensive framework for quantitative control of transmission risk using all available air cleaning mechanisms in an indoor space while minimizing energy costs to aid in the design and automated operation of healthy, energy-efficient buildings.

1. Introduction

The COVID-19 pandemic disrupted the global economy and caused the worldwide shut-down of many public and private buildings essential for daily life, including schools, gyms, religious centers, and offices [1]. At first, public health guidance focused on limiting transmission from fomites and exhaled large droplets, via surface disinfection and social distancing (such as the 6 foot rule), respectively [2]. As the pandemic continued, however, it was recognized that a dominant mode of transmission of COVID-19 is through virus-laden exhaled aerosol droplets, which are small enough to remain suspended in the air for minutes to hours and become well-mixed across indoor rooms [3–8], so the recommended mitigation strategies shifted from social distancing to masking and improved ventilation and filtration of indoor air [9–11]. Notably, a collection of leading experts in respiratory disease transmission and building science called for a "paradigm shift" in the design and operation of indoor air control systems, analogous to historical efforts to reduce pathogen transmission through food and water sources [12], as healthy indoor air is becoming recognized as a fundamental human need [13].

In this work, we propose a physics-based, data-driven strategy to achieve this paradigm shift in healthy buildings, which integrates mathematical models of airborne disease transmission with available building data streams, and apply it to data collected from multiple buildings and indoor space types. By combining airflow measurements from building management systems (BMS) with CO_2 concentration data and other measures of indoor air quality (IAQ) obtained from portable sensors, the underlying physics-based models are calibrated and used to simulate the transmission risk and energy consumption for each indoor space, as operated. We validate the use of simple, pseudo-steady models for airborne transmission rates and then integrate these models within a control framework to directly control for transmission rate in an energy-efficient manner. Using our workflow, public health officials can quantitatively assess mitigation strategies for indoor airborne disease transmission and recommend novel building control protocols to limit transmission while minimizing energy costs. Such quantitative analysis

* Correspondence to: 617.324.2036, 77 Massachusetts Ave, Cambridge, MA 02139, United States of America.
E-mail address: bazant@mit.edu (M.Z. Bazant).
[1] Contributed equally to this work.

https://doi.org/10.1016/j.buildenv.2023.110893
Received 23 May 2023; Received in revised form 26 September 2023; Accepted 30 September 2023
Available online 10 October 2023

and automated building controls is necessary for developing healthy buildings to minimize the transmission of airborne diseases.

2. Methods

2.1. Experiment

We collected data from diverse indoor spaces on the Massachusetts Institute of Technology (MIT) campus for several weeks in April 2022. College campuses have highly varying occupancy and a variety of room types and sizes, from large lecture halls to small offices, thereby creating an ideal environment for testing IAQ control measures. The monitored spaces are all served by heating, ventilation, and air-conditioning (HVAC) systems, which include sensors to measure and record total supply airflow, outdoor airflow, and supply air temperature. Temporary in-room Kaiterra sensors were also deployed to collect additional measurements relevant to IAQ, including temperature, relative humidity, CO_2 concentration, total volatile organic compounds (TVOC), PM10, and PM2.5. Only the first three measurements are used in this study, but the entire dataset is publicly available (SI 6). To measure outdoor temperature and humidity, which are relevant for estimating the energy consumption associated with ventilation, a QuantAQ sensor was placed on the roof of one of the monitored buildings. This sensor also provides size-resolved measurements of particulate concentrations, but those data streams were not used in this study. In addition, we collected information about each room, including floor area, ceiling height, use case, design occupancy, and HVAC configuration (SI 1).

The overall workflow for this study is illustrated in Fig. 1. The key idea is that all data streams are integrated with physics-based models to predict and control transmission risk and energy consumption. This data fusion ensures that all space-specific variables in the model are known or accurately estimated, thus allowing different spaces to be compared with confidence. Example time series data for four of the monitored rooms are shown in Fig. 2 and exhibit variations on the scales of days, hours, and minutes. The CO_2 and humidity measurements come from the in-zone IAQ sensors, while outdoor-airflow measurements come from the BMS or are estimated from CO_2 measurements. Of these measurements, CO_2 concentration is the most strongly varying, as it is driven primarily by room occupancy. The peak values for Classroom 3 are significantly higher than for the other rooms, as it is does not have a forced supply of outdoor air provided by the HVAC system and is thus only naturally ventilated.

Note that the term "ventilation" is often defined broadly to include all treated air delivered to a space [14], i.e., including filtered recirculated air. However, almost all the spaces monitored are served by dedicated outdoor-air systems, which means "ventilation" is exclusively provided via outdoor air. In the interest of brevity, we use the term "ventilation" to refer specifically to *outdoor-air* ventilation throughout this discussion. Where relevant, recirculation and other airflows are handled separately.

2.2. Theory

2.2.1. Infectious particle model

Simple mass-balance models [15,16] have been used for decades to study airborne transmission via aerosols and have been successfully applied to explain transmission in prior diseases [17,18] and COVID-19 [9,19–22]. Each room is assumed to be well-mixed, such that the particle concentration can be treated as uniform throughout the room [15,23]. This assumption is shown to produce high-quality occupancy estimates, indicating sufficient accuracy for our purposes. The mass balance for infectious particles in a room results in the following partial differential equation model for the time-evolution of infectious pathogen concentration, $C(r,t)$, per droplet size in a room of volume V and area A [9]:

$$V\frac{\partial C(r,t)}{\partial t} = N_i(t)P(r) - \left(Q_a + p_f(r)Q_r + v_s(r)A + \lambda_v(r)V + \sum_d p_d(r)Q_d\right)C(r,t). \quad (1)$$

where N_i are the number of infectors present in the room exhaling infectious droplets with rate P (SI 2). Infectious droplets are removed through outdoor airflow (Q_a), filtration in the recirculated airflow ($p_f(r)Q_r$), sedimentation ($v_s(r)A$), deactivation ($\lambda_v(r)V$), and the action of disinfection devices ($\sum_d p_d(r)Q_d$). All removal mechanisms can be expressed as rates, $\lambda_a = Q_a/V$, $\lambda_f(r) = p_f(r)Q_r/V$, $\lambda_s(r) = v_s(r)A/V$, and $\lambda_d(r) = \sum_d p_d(r)Q_d/V$, and lumped into a single parameter that describes the supply of "equivalent outdoor air" (EOA) delivered to the space, $\lambda_{\text{EOA}} = \lambda_a + \lambda_f + \lambda_s + \lambda_v + \lambda_d$ [24]. EOA quantifies each removal mechanism in terms of volumetric flow of outdoor-air ventilation that would lead to an equivalent removal rate of infectious particles, thus facilitating comparisons among disparate processes.

The recent ASHRAE Standard 241 [25] defines a quantity "equivalent clean airflow" that is the same as EOA except that the passive mechanisms (sedimentation and deactivation) are not included (i.e., $\lambda_{\text{ECA}} = \lambda_1 + \lambda_f + \lambda_d$). We use EOA in this paper as it is more relevant for directly modeling transmission risk. As we will show later, the resulting control strategies are responsible for meeting a (possibly time-varying) target of EOA delivery, which is consistent with the approach of ASHRAE 241.

2.2.2. Safety guideline

Following [9], the model can also be approximated analytically to derive a "safety guideline" that provides the correct relationships for how disease and building parameters relate to infection risk. The guideline bounds the indoor reproductive number, $\mathcal{R}_{\text{in}}$, defined as the expected number of transmissions if an infector were present for a time τ in a given room:

$$\mathcal{R}_{\text{in}} = Q_b^2 p_m^2 C_q \frac{N_s \tau}{\lambda_{\text{EOA}}(\bar{r})V} < \epsilon. \quad (2)$$

where C_q represents the infectious quanta concentration in exhaled air (SI 3); Q_b is the occupants' breathing rate; p_m is a mask penetration factor of aerosols; V is the volume of the room; N_s is the number of susceptible occupants; and ϵ is the desired risk tolerance. Droplet size dependencies are integrated out by defining an effective droplet size $\bar{r}$ (SI 3). If $\mathcal{R}_{\text{in}}$ for a specific indoor space is below an appropriate tolerance, the space will not contribute to disease spread. Therefore, Eq. (2) provides building operators with a guideline for setting building-specific parameters to safe values, given measurements of disease-specific parameters. Typical ranges for these parameters and the values used in this study are provided in Supporting Information (SI 7).

Simply put, $\mathcal{R}_{\text{in}}$ is proportional to the product of susceptible occupants and the time spent, divided by the EOA provided to the room. Thus, any holistic risk assessment and transmission mitigation strategy must consider all three dimensions. For example, simply mandating a maximum occupancy in an indoor space may not adequately reduce transmissions if the occupants spend a large amount of time in the space. Alternatively, occupancy limits may be unnecessary, if an appropriate amount of EOA is delivered to the space. The guideline is intended to be used to compare the relative magnitude of how different interventions, such as requiring mask usage or increasing building ventilation, impact transmission. Setting a strict ϵ threshold requires population-based studies of all indoor spaces in a community.

2.2.3. CO_2 -based Safety Guideline

CO_2 is often used as an indicator of transmission risk [26–29], but we stress that it is only a partial proxy that requires care to interpret, especially when comparing across spaces with significantly

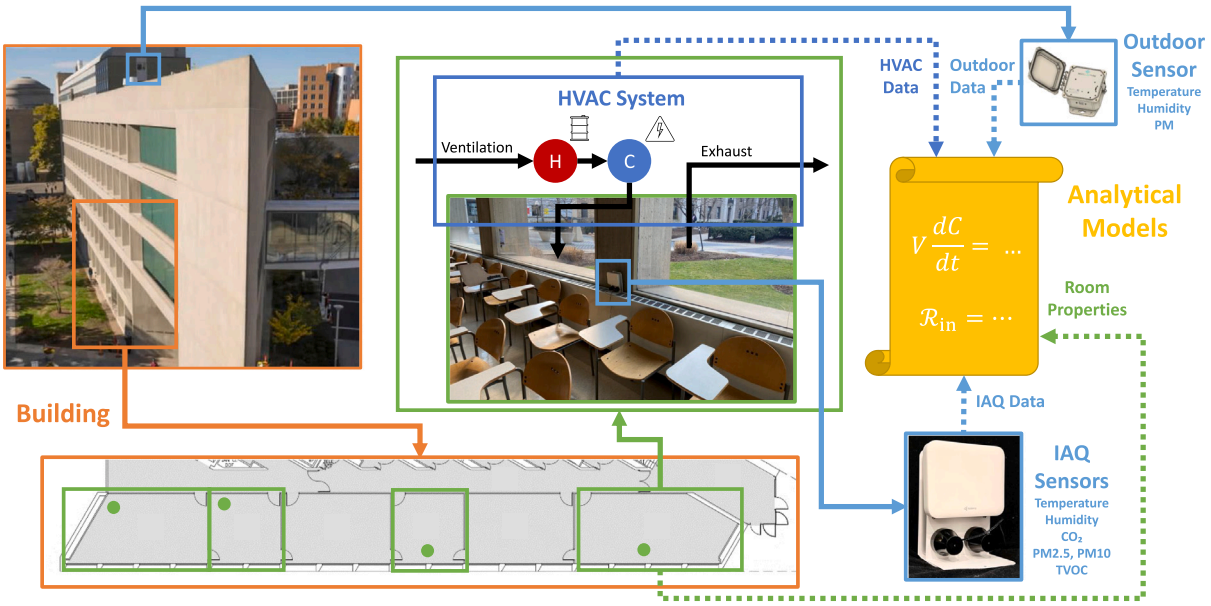

Fig. 1. Diagram of overall workflow. Portable indoor air quality (IAQ) sensors are placed in each monitored room, and a more durable sensor is placed on the roof to record outdoor conditions. These sensor measurements are then combined with time-series data from the heating, ventilation, and air conditioning (HVAC) system and basic properties of each room (area, ceiling height, design occupancy, etc.) for analysis.

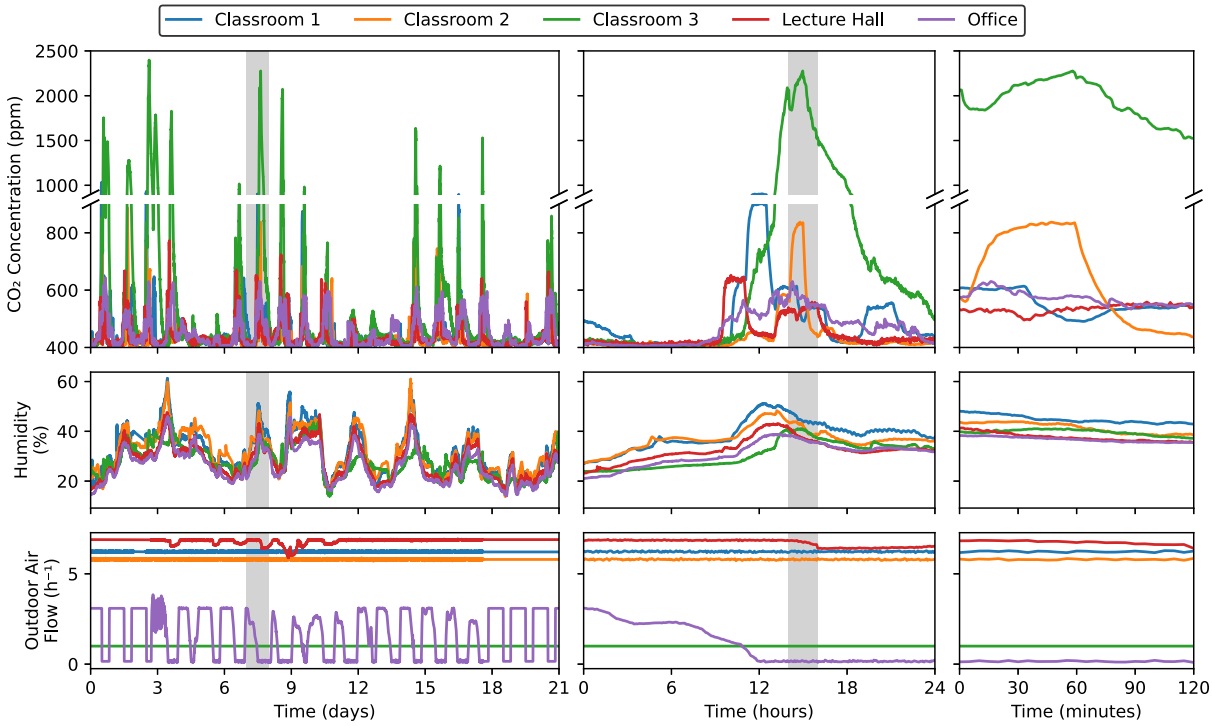

Fig. 2. Plot of sample time series data from the study period at multiple time scales (days, hours, and minutes). The shaded region in the first (or second) column shows the time range covered in the second (or third) column. Missing data points have been filled in via interpolation.

different HVAC systems. In particular, the dynamical model for CO_2 concentration, C_{CO_2}, is

$$\frac{dC_{CO_2}}{dt} = \frac{Q_b}{V} C_{CO_2,b} N_t(t) - \lambda_a (C_{CO_2} - C_{CO_2,OA}), \tag{3}$$

where Q_b is the occupant breathing rate (which can be estimated based on age and activity level [30]), $C_{CO_2,b}$ is the exhaled-breath excess CO_2 concentration, $N_t(t)$ is the time-dependent room occupancy, and $C_{CO_2,OA}$ is the outdoor-air CO_2 concentration. To derive a CO_2-based guideline, a pseudo-steady analysis of the dynamical model for CO_2 concentration can be combined with Eq. (2) [27], which incorporates the differences between infectious particle dynamics and CO_2 dynamics stemming from sources of EOA beyond outdoor-air ventilation. We thus arrive at the following safety guideline based on CO_2 concentration measurements:

$$(C_{CO_2,s} - C_{CO_2,OA})\tau < \epsilon \frac{C_{CO_2,b}}{Q_b p_m^2 C_q} \frac{\lambda_{EOA}(\vec{r})}{\lambda_a} \tag{4}$$

Critical in this formulation is the term λ_{EOA}/λ_a, which is necessary to account for the sources of EOA other than outdoor-air ventilation. In

particular, it means the CO_2 concentrations *cannot* be directly compared across spaces as a proxy for transmission risk unless it is known that the underlying EOA sources are in the same proportion.

2.2.4. Short-range transmission

Short-range respiratory flows also contribute to the risk of disease transmission in indoor spaces [31–33] and should be compared with the risk of long-range airborne transmission in any safety guideline [9].

Estimates of short-range transmission rates can be derived from the theory of turbulent jets [9]. This analysis predicts that the concentration of infectious particles in the jets of infectors' exhaled breath decays as $1/x$ where x is horizontal distance. A key deficiency of this model is that it does not account for the buoyancy of exhaled breath, which causes it to quickly rise out of the breathing zone of a potential susceptible person. Thus, rather than use the turbulent jet models directly, we instead employ an empirical model derived from the experimental results of [34]. In this paper, the authors calculate a "susceptibility index" defined as $\epsilon := C(x)/C_\infty$ where $C(x)$ is the infectious particle concentration at horizontal distance x from the mouth of the infector, and C_∞ is the background room concentration. For our purposes, we assume the concentration within the jet follows the model

$$\theta := \frac{C(x) - C_\infty}{C_b - C_\infty} \approx \frac{k}{x} \tag{5}$$

where k is an unknown constant to be determined. Assuming $C_\infty = C_b Q_b / V\lambda_{\text{EOA}}$ follows the pseudo-steady well-mixed model, we can derive the relationship

$$\theta = \frac{(\epsilon - 1)Q_b}{V\lambda_{\text{EOA}} - Q_b} \tag{6}$$

To quantify the short-range transmission risk, we use the model

$$\mathcal{R}_{\text{short}} = Q_b C(x) p_{\text{short}} \tau \tag{7}$$

in which the new parameter p_{short} represents the probability that a susceptible is directly within the short-range plume exhaled by each infector. Note the similar form to the well-mixed formulation (2), with the primary difference that the short-range risk depends on occupant separation distance x. More information about how we determine this parameter is provided in SI 4.

2.2.5. Occupancy and ventilation estimation

A key factor affecting the transmission rate is the time-varying occupancy in each space, which is then used to estimate the numbers of susceptible, N_s, and infectious, N_i, occupants. There are various occupant-counting technologies available, which utilize combinations of different time series measurements and prediction algorithms. Physical approaches for estimating occupancy involve formulating a model for CO_2 concentration evolution, and solving an inverse problem constrained by the model for the time-varying occupancy to fit a measured CO_2 time series [35–41]. Black box approaches involving statistical and machine learning approaches, including neural networks, support vector machines, and multiclass classification have also been employed to estimate time-varying occupancy using CO_2 data alone [36,42] and CO_2 data along with other environment measurements including temperature, humidity, light, motion, and sound [43–47]. Depending on the data that the method uses, the required equipment may be expensive and complicated to install, so many spaces will not have occupancy counts directly available. In addition, many of these technologies may compromise the privacy of occupants by using video or images of occupants. Finally, machine learning methods which utilize multiple streams of environmental data often require individual training data for each room, which is infeasible to apply to a large number of rooms. One alternative would be to simply assume a fixed occupancy count and time-varying schedule (e.g., as provided by [48]) for each space, but this approach would likely introduce unacceptably high error, especially when occupancy is highly variable. Given these challenges, we thus estimate occupancy by modifying previous methods that solve the full inverse problem of the CO_2 concentration dynamical model given by Eq. (3) and data, with a novel extension to simultaneously estimate ventilation rates if not measured. This method protects occupant privacy and requires no training data, so it can be easily implemented in new spaces.

When the outdoor-air ventilation rate $\lambda_a(t)$ is known (e.g., due to direct measurement or correlation with other available measurements [49,50]), we can estimate occupancy $N_t(t)$ by choosing a set of basis functions and finding the linear combination of those basis functions such that the predicted time series of C_{CO_2} under (3) matches the actual measured values as closely as possible. This step is performed by embedding a discretized version of this model inside an optimization problem and solving for the basis-function coefficients via optimization techniques. Mathematically, we denote the basis functions $\phi_i[t]$ for N_t. To embed the model, we choose a fixed sample rate $\Delta = 1$ min and define a new function $f(C_{CO_2}, N_t, \lambda_a)$ to give the explicit Runge–Kutta 4 discretization of the ODE model (3). The resulting optimization problem is thus

$$\begin{aligned} \min_{\alpha_1,\dots,\alpha_I} \quad & E := \sum_t \left| C^m_{CO_2}[t] - C_{CO_2}[t] \right|^2 \\ \text{s.t.} \quad & C_{CO_2}[t+1] = f(C_{CO_2}[t], N_t[t], \lambda_a[t]) \\ & N_t[t] = \sum_{i=1}^{I} \alpha_i \phi_i[t] \\ & N_t^{\min} \le N_t[t] \le N_t^{\max} \end{aligned} \tag{8}$$

given CO_2 concentration measurements $C^m_{CO_2}[t]$ and pre-defined occupancy bounds $N_t^{\min}$ and $N_t^{\max}$ (which we set respectively to zero and 1.5 times each room's design occupancy). Note that we use square brackets to emphasize that these quantities are defined in *discrete* time. Because the function $f(\cdot,\cdot,\cdot)$ is *linear* in its first and second variables, the resulting optimization problem is thus a convex quadratic programming problem that can be solved using standard techniques.

In cases where the ventilation rate $\lambda_a(t)$ is *not* measured or otherwise known, the proposed strategy requires some modification. One possible method to estimate its value would be to add corresponding basis functions for $\lambda_a[t]$ and embed them in the optimization problem with new decision variables analogous to the treatment of N_t. For spaces with sufficiently low ventilation rates (and sufficiently high sample rate for CO_2 concentration measurements), this modification can be sufficient, with the resulting ventilation and occupancy estimates being the ones that most closely match the measured CO_2 data. However, this change would render the resulting optimization problem nonconvex, and selection of appropriate basis functions could be challenging. In addition, if there are few changes in occupancy throughout the day, the chosen objective function is dominated by pseudo-steady periods with $dC_{CO_2}/dt \approx 0$, which thus implies the degenerate relationship $\lambda_a \propto N_t$ and creates additional problems as discussed below. Therefore, we instead opt for a slightly different approach.

We begin by assuming that the outdoor-air ventilation rate $\lambda_a(t)$ is *constant* over the time horizon with value $\bar{\lambda}_a$ to be determined. We then let $E(\bar{\lambda}_a)$ denote the optimal value of the optimization problem (8) assuming $\lambda_a[t] \equiv \bar{\lambda}_a$, and we let $N_t[t](\bar{\lambda}_a)$ denote the corresponding value of the occupancy profile. To estimate $\bar{\lambda}_a$, we can thus solve the one-dimensional optimization problem

$$\min_{\bar{\lambda}_a} \quad E(\bar{\lambda}_a) \quad \text{s.t.} \quad \lambda_a^{\min} \le \bar{\lambda}_a \le \lambda_a^{\max} \tag{9}$$

by using the volume-normalized λ_a as the decision variable, as we know its value should almost always be between 1 and 10 h^{-1} independent of the specific room. Thus, despite its nonconvexity the problem can be solved by simple bounded scalar optimization techniques, or even via an exhaustive grid search with a chosen granularity. To estimate uncertainty in the estimate we take a level set of the objective function, with the threshold set to 50% higher than the optimal value $E(\bar{\lambda}_a^*)$.

If there are a sufficient number of large occupancy changes, this procedure can produce a tight range for the estimated ventilation, primarily by matching the exponential decay predicted by the model during such events to the measured data. However, if occupancy is relatively constant, the data will be dominated by the pseudo-steady relationship

$$C_{\mathrm{CO_2}} - C_{\mathrm{CO_2,OA}} = \frac{Q_b C_{\mathrm{CO_2},b} N_t}{\lambda_a V} \tag{10}$$

which is linearly degenerate, so the resulting uncertainty region will be extremely large. Similarly, there may be uncertainty in the breathing rate Q_b, especially in spaces with significant variance in age or activity level [30].

To break this degeneracy, we note that while we certainly do not know the full time-varying occupancy profile, we often have a good idea of *peak* occupancy $\hat{N}_t$ over the given time period. Letting $\mathcal{N}_p(\bar{\lambda}_a)$ denote the pth percentile of the occupancy estimates $N_t[t](\lambda_a)$, we thus desire that $\mathcal{N}_{95\%}(\bar{\lambda}_a) \approx \hat{N}_t$. (We use the 95th percentile to add some degree of robustness to small periods of abnormal data, e.g., when the HVAC system is shut down for maintenance.) Adding this relationship to the cost function, we thus arrive at our final modified optimization problem

$$\min_{\bar{\lambda}_a} \quad E(\bar{\lambda}_a) + \mu(\bar{\lambda}_a)\left|\mathcal{N}_{95\%}(\bar{\lambda}_a) - \hat{N}_t\right| \quad \text{s.t.} \quad \lambda_a^{\min} \le \bar{\lambda}_a \le \lambda_a^{\max} \tag{11}$$

in which $\mu(\cdot)$ is a scaling factor to weigh the two terms. We use

$$\mu(\lambda_a) := 0.05\frac{Q_b C_{\mathrm{CO_2},b}}{\lambda_a V}$$

so that this penalty accounts for (5% of) the error that would be induced in the pseudo-steady model due to the difference in occupancy. In practical applications, this scale factor would be adjusted up or down depending on confidence in the assumed peak occupancy $\hat{N}_t$. For each room, the assumed value of $\hat{N}_t$ is generally set equal to 50%–100% of design occupancy consistent with typical usage during the monitoring period.

Finally, some buildings may be in an intermediate case where, despite a measurement of the mechanically-provided outdoor airflow, there is a significant *unmeasured* portion due to infiltration and air leakage. These sources of outdoor air do have a noticeable impact on energy consumption, and the magnitude varies significantly based on building construction and other factors [51]. In the context of EOA delivery, the resulting airflow may be small enough to neglect (simulations suggest infiltration rates near 0.1 $\mathrm{h^{-1}}$ in offices and 0.25 $\mathrm{h^{-1}}$ in schools [52]), especially when using the CO_2-based formulation (4) where the errors would largely cancel out. Nevertheless, it is possible to modify the procedure above to directly estimate the leakage rate from measured data [53]. Specifically, the total outdoor-air rate λ_a in (8) should be decomposed as $\lambda_a[t] = \lambda_a^m[t] + \tilde{\lambda}_a$ in which $\lambda_a^m[t]$ is the measured portion, and $\tilde{\lambda}_a$ is the leakage rate to be estimated. $\tilde{\lambda}_a$ is then optimized as above in (11). As pointed out in previous studies [54,55], accuracy is best when the data contains transitions to zero occupancy, as the resulting exponential decay in CO_2 concentration gives the effective leakage rate. Fortunately, leakage rates are generally lower during occupied hours when the HVAC system is active [48,52], so extreme accuracy is not necessary when there are other more significant sources of EOA.

2.2.6. Transmission-controlled ventilation

While addressing public health concerns, there are still many opportunities to reduce energy consumption in buildings, which account for 40% of total energy use in the United States [56]. Long term building operation must balance airborne transmission risk and IAQ with energy consumption.

Formulating all removal processes in terms of EOA provides a common basis to compare various technologies in terms of cost per 1 $\mathrm{h^{-1}}$ of EOA. Under this lens, filtration, which can either be provided by in-room air cleaners or recirculated supply air, is often a much more energy-efficient source of EOA than outdoor-air ventilation. As an alternative, ultraviolet (UV) light can provide significant EOA by eradicating any infectious material within particles [57–60] and can be installed in an upper-room configuration with shielding or as "far-UV" that is not harmful to occupants [61]. If properly installed, such systems can deliver EOA even more efficiently than filtration-based sources [62]. Thus, to optimize energy efficiency, it is necessary to consider all of these options.

Unfortunately, the primary source of EOA for many rooms is in fact outdoor-air ventilation. Considering the large variance in transmission risk for spaces with strongly time-varying occupancy, however, it is possible to significantly reduce energy costs by limiting extra ventilation to periods of high occupancy. Here, we analyze and compare demand-controlled ventilation (DCV) and transmission-controlled ventilation (TCV) operation modes. DCV is a feedback control mechanism implemented in many modern HVAC systems (11% of office buildings and 21% of educational facilities in the US [63]) that adjusts ventilation rates in real time to maintain a setpoint of CO_2 concentration. This method thus does not consider any other EOA sources, and thus the mapping from CO_2 setpoint to transmission risk can vary strongly from space to space. However, given that our primary goal is to control the transmission risk in each room, we propose TCV as a novel operating mode to maintain a transmission-rate setpoint by interfacing with HVAC and accounting for other sources of EOA, all of which impact airborne disease transmission.

To implement this control strategy, we first need to evaluate the current transmission rate $\dot{\mathcal{R}}_{\mathrm{in}} := \mathcal{R}_{\mathrm{in}}/\tau$. The pseudo-steady model gives $\dot{\mathcal{R}}_{\mathrm{in}} := Q_b^2 C_q N_s / \lambda_{\mathrm{EOA}} V$. The value of $\lambda_{\mathrm{EOA}} V$ can be calculated using flow measurements and filtration parameters for the BMS-provided clean air and the humidity measurements and physics-based models for the deposition and deactivation components of EOA. To avoid the need for an explicit estimate of N_s, we define the CO_2 generation rate as $g_{\mathrm{CO_2}} := Q_b C_{\mathrm{CO_2},b} N_t / V$ and make the (conservative) assumption that $N_s \approx N_t$. We thus arrive at the formula

$$\dot{\mathcal{R}}_{\mathrm{in}} = \frac{Q_b C_q}{\lambda_{\mathrm{EOA}}} \frac{g_{\mathrm{CO_2}}}{C_{\mathrm{CO_2},b}} \tag{12}$$

which can be evaluated by the BMS. The primary benefit is that $g_{\mathrm{CO_2}}$ can be estimated directly from successive measurements of $C_{\mathrm{CO_2}}$ and λ_a in accordance with the dynamic model (3).

To define the action of the controller, we thus take a transmission-rate setpoint $\dot{\mathcal{R}}_{\mathrm{in}}^{\mathrm{sp}}$ (chosen in accordance with expected exposure time τ) and invert the previous formula to find the corresponding EOA setpoint

$$\lambda_{\mathrm{EOA}}^{\mathrm{sp}} := \frac{Q_b C_q g_{\mathrm{CO_2}}}{\dot{\mathcal{R}}_{\mathrm{in}}^{\mathrm{sp}} C_{\mathrm{CO_2},b}} \tag{13}$$

From this value, the BMS can adjust its various setpoints to deliver the required amount of EOA. In cases where the BMS can control multiple sources of EOA (e.g., outdoor-air ventilation, filtration via recirculation, and possibly in-zone disinfection devices), some form of prioritization would be needed, for example selecting in order of increasing energy consumption. We note also that the proposed TCV strategy does not replace and must be applied in addition to current ventilation controls as required by ASHRAE 62.1 [14]. More information on the corresponding control logic is provided in SI 5.

3. Results

3.1. Occupancy and ventilation estimation

To validate the proposed approach for occupancy estimation, we manually collected a limited amount of occupancy data in two rooms, as shown in Fig. 3. In Classroom 1, attendance was taken at each class, which was assumed to be constant throughout the 90-minute lecture period. In Office, a sign-in/sign-out sheet was used over a three day

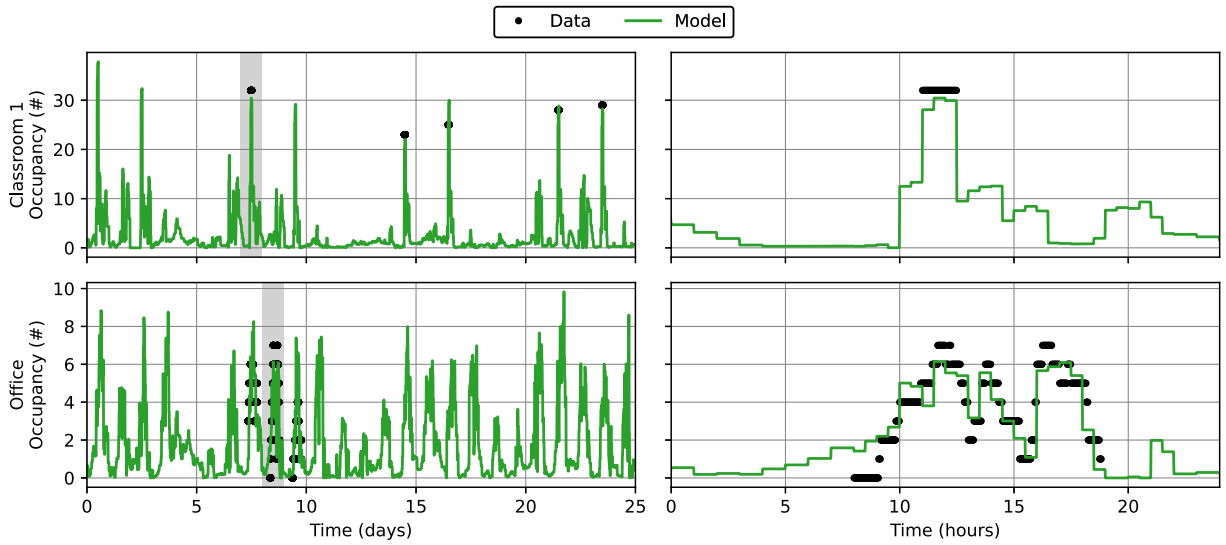

Fig. 3. Fit occupancy profiles for rooms with (partial) occupancy data. Occupancy is assumed to be constant over each 30-minute interval in the optimization formulation. Despite simplicity of the well-mixed models, estimated occupancy profiles closely match the available occupancy data.

period to estimate time-varying occupancy. Fig. 3 shows the estimated time-varying occupancy in both rooms throughout the monitoring period, as determined by the solution to (8). During nominal occupied hours, we see that the estimates are in good agreement with measured occupancy where available. Daily root-mean-square error ranges from 1.8 to 3.9 occupants (7% to 16%) for Classroom 1 and 0.9 to 1.6 occupants (22% to 37%) for Office, consistent with performance using similar methods in the literature [36]. In addition, we note the strong time-varying character of these curves, which emphasizes the need to use realistic occupancy profiles (rather than simple fixed schedules) to accurately assess transmission risk for these spaces. Additional validation in other spaces is certainly warranted as future work, but this performance is good enough for our purposes.

To illustrate the proposed approach for simultaneous occupancy and ventilation estimation, Fig. 4 shows the objective functions, model fits, and estimated occupancy profiles for a 1-day period in Classroom 1. Note that the gray "CO_2 Fit" objective corresponds to the formulation in (9), while the black "+Occupancy Penalty" is the modified formulation in (11). As mentioned before, uncertainty regions are calculated as ±50% of the optimal objective value. Including only the penalty on CO_2 concentration fit, we see that the estimated outdoor-air ventilation rate is quite low, with a large relative uncertainty. Although the CO_2 error rules out the extremely low and high ventilation rates, it cannot adequately distinguish between the intermediate values. However, after adding the additional term for deviation from the peak occupancy target (set to 70% of the room's design occupancy), the estimated value is now much closer to the actual measured value, with lower relative uncertainty. We use this same strategy to estimate time-varying occupancy profiles for the remaining spaces (assuming 70% peak occupancy in classrooms, 50% in lecture halls, and observed values for office spaces, all of which are consistent with operating policy at the time of data collection).

3.2. Infection risk

The workflow can be assessed by calculating the transmission risk in the different indoor spaces using the collected data along with the full dynamical model and the pseudo-steady approximation. The transmission rate values predicted by the full model and pseudo-steady approximation are in excellent agreement, and where they differ, the pseudo-steady model produces more conservative estimates (Fig. 5). We assess these models in two ways. In Fig. 5, we extract random segments of data from Classroom 2 (during nominally occupied hours) and plot points for each segment on a plane with axes for average occupancy and time. The color of each point corresponds to the event reproductive number calculated from the full dynamical model. Since EOA delivery is essentially constant for this space, the pseudo-steady model predicts that $\mathcal{R}_{in} \propto$ Occupancy × Time, which is the same trend exhibited by the color of the points in Fig. 5. This validates the use of the safety guideline, Eq. (2), to limit occupancy and time such that $\mathcal{R}_{in}$ is below a given tolerance, as indicated by the dashed curve, which can be shifted by altering the amount of EOA provided in the room.

To assess other spaces, Fig. 5 shows distributions of transmission rates across all the monitored spaces. These points are based on a 5-minute sample rate for both models, and the distributions are weighted by the number of occupants within each point. The black dots indicate the corresponding steady-state transmission rate for a space of that type with baseline ventilation rates and occupant density, per ASHRAE standards. We see that, in almost all spaces, the worst-case transmission rate is below the baseline value as expected, since MIT buildings were deliberately operated with extra ventilation during the monitoring period to limit COVID-19 transmission. Again, the distribution of transmission rates calculated from the pseudo-steady model (gray curves) closely matches the distribution of transmission rates calculated from the full dynamic model (green curves). The median values of these distributions are generally within 1% agreement, and the maximum values differ by less than 10%.

The primary outlier from this trend is Classroom 3*, which has no mechanical ventilation, resulting in significantly smaller EOA delivery than in the other spaces. As a result, when a large number of people enter this room, the infectious particle concentration takes longer to approach the pseudo-steady values. As such, the pseudo-steady model predicts a more conservative, higher transmission rate. When a large number of people leave those spaces, the opposite transient effect occurs, but since the occupancy is generally lower as people are leaving the space, those events are weighted less in the final distribution. The net result is that the pseudo-steady model predictions are slightly conservative.

The results shown for Classrooms 3 and 3* are for the same space, occupancy profile, and ventilation rate, but different levels of filtration. We assume an active filter delivering 4.5 h^{-1} of HEPA filtration in Classroom 3 and inactive filter in Classroom 3*. When the filter is inactive, there is roughly a threefold increase in median transmission rate. We highlight this distinction because measured CO_2 concentrations would be exactly the same for the two scenarios, since filtration is a form of EOA that does not impact CO_2, which thus cannot be used by itself to assess transmission risk. Instead, safety guidelines [9,27],

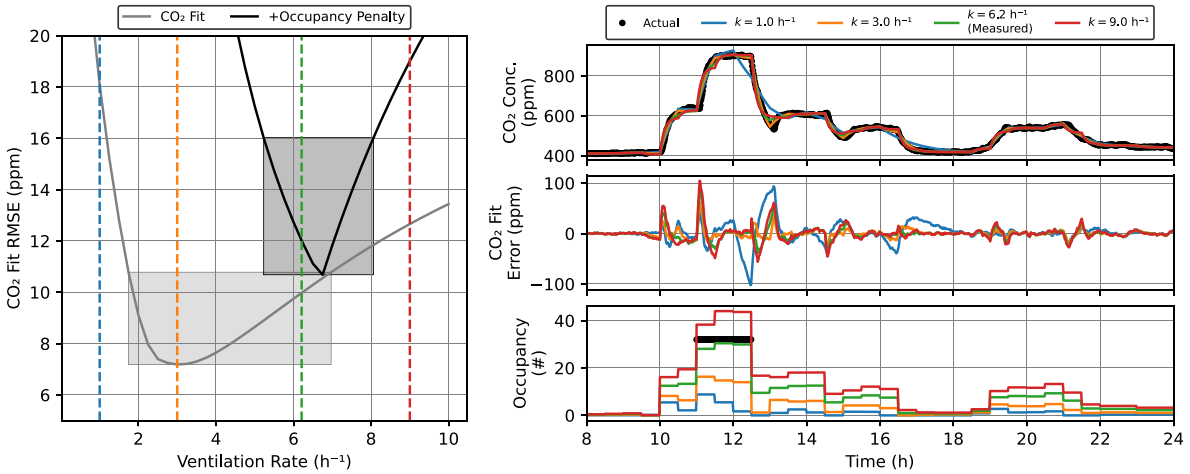

Fig. 4. Simultaneous estimation of outdoor-air ventilation rate and time-varying occupancy. Left: objective function with (black) and without (gray) the peak-occupancy penalty along with uncertainty regions. The optimization procedure chooses the ventilation rate with the lowest value of these objective functions. Right: simulated CO_2 concentrations, fit errors, and estimated occupancy for selected ventilation rates. These values correspond to the dashed colored lines on the left. Note that the measured ventilation rate for this room was 6.2 h^{-1}, which corresponds to the green curves. (For interpretation of the references to color in this figure legend, the reader is referred to the web version of this article.)

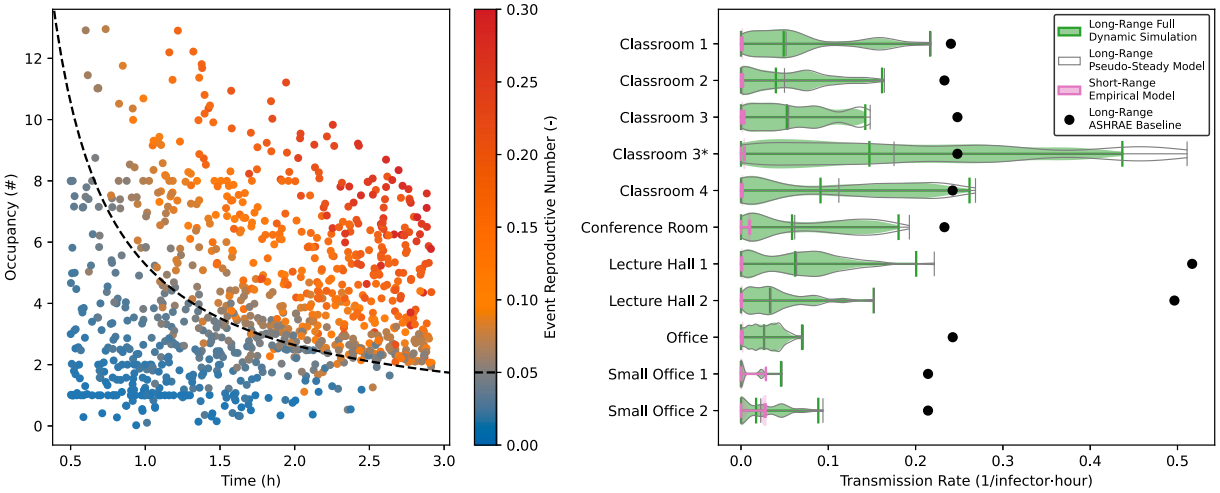

Fig. 5. Transmission predictions for selected rooms in the study. Left: Scatter plot of the reproductive number for randomly chosen time periods from the full dynamical simulations, found to be in good agreement with the safety guideline [9] from the pseudo-steady formula, Eq. (2). Right: Distributions of transmission rates throughout the study period computed using full model simulation and pseudo-steady approximation, again showing good agreement. The distributions are weighted by occupancy and thus predict the expected number of transmissions if one occupant were to be infectious for one hour. Green curves are the distributions from the full dynamic model, with green lines showing the minimum, median, and maximum values. Gray curves are the distributions from the pseudo-steady model, with gray lines showing the same three statistics. Black dots show expected values assuming minimum ventilation rates and occupant density per ASHRAE standard 62.1 [14]. (For interpretation of the references to color in this figure legend, the reader is referred to the web version of this article.)

which incorporate the differences between total EOA and outdoor-air ventilation, based on a fixed $\mathcal{R}_{in}$ tolerance, are more appropriate to account for differences in indoor spaces.

We also conservatively estimate that for most of the spaces monitored, short-range effects (pink curves) account for less than 5% of the expected transmissions caused by long-range mixing using Eq. (7). The only exception is for rooms where close-range face-to-face contact between occupants is common, such as in the Small Office spaces, where short-range risk may reach up to 30% of the long-range risk. However, the flows responsible for short-range transmission can be eliminated by requiring occupants to wear masks [64].

3.3. Energy and control analysis

Given a desired level of total transmission risk, buildings should operate to achieve that risk as efficiently as possible, taking advantage of all available mechanisms of infectious particle mitigation. Here, we analyze and compare DCV and TCV, our novel control strategy, operation modes.

To quantitatively assess the inherent tradeoff between energy consumption and transmission risk, we estimate the daily energy cost for each room as operated and under various hypothetical scenarios using standard thermodynamic and equipment modeling procedures from our previous work [65,66]. Heating and cooling energy is calculated from measured flow, supply temperature, and outdoor air temperature (assuming a COP of 3 for mechanical cooling and 90% efficiency for gas heating). Fan power is estimated from measured flow and an assumed fan curve. Costs are calculated assuming fixed prices of 0.12 $/kWh for electricity and 8 $/MMBTU for gas. For the monitored rooms, the primary cost driver is the energy required to heat the outdoor air up to its supply temperature.

We refer to the actual operation during the monitoring period as the "Baseline" scenario. The hypothetical scenarios considered for each room are as follows:

- Curtailed: ventilation is supplied at the same rate as observed in the data only during nominal occupied hours, assumed to be 8 am through 10 pm.
- Minimum: ventilation follows the "Curtailed" schedule and is further adjusted to provide the minimum amount of ventilation required in each space per ASHRAE standard 62.1 [14].
- In-Zone Filtration: in addition to the "Minimum" scenario, supplemental in-room filtration is provided via standalone air cleaners (active during occupied hours) such that total EOA delivery meets the threshold set by ASHRAE standard 241 [25].
- In-Zone Far UV: as above except that the additional EOA is provided by upper-room far UVC lamps.
- Demand Controlled (DCV): ventilation is provided by a standard demand control algorithm for a given CO_2 concentration setpoint.
- Transmission Controlled (TCV): ventilation is provided by a modified algorithm that provides enough ventilation to operate below a given transmission risk as calculated by the pseudo-steady model.
- TCV + Far UV: ventilation is provided by TCV alongside the additional EOA delivered in the "In-Zone Far UV" case.

Note that the "In-Zone Filtration" and "In-Zone Far UV" scenarios are chosen to be in compliance with ASHRAE 241 assuming occupancy limits consistent with operation at the time of data collection.

After estimating the time-varying ventilation that would be provided by each hypothetical strategy, transmission risk and energy cost can be calculated using the modeling approach discussed previously. These results are shown for three representative spaces in Fig. 6. Similar plots for other spaces are provided in the Supporting Information.

In all spaces in Fig. 6, we see there are significant opportunities to reduce energy consumption without large changes in the average and spread of the transmission rate. Simply curtailing ventilation during nighttime unoccupied hours cuts energy consumption roughly in half, with only a slight increase in transmission rate due to a small number of after-hours gatherings in that room. The ASHRAE minimum protocol further reduces energy consumption but increases the mean and spread of the transmission rate. Adding in-room filtration can reduce transmission below baseline values and satisfy ASHRAE 241 while still providing significant reduction in energy cost. Based on current experimental data [61], far UV disinfection is even cheaper than in-room filtration to achieve similar EOA delivery. However, by applying some of the more advanced control algorithms, transmission rate can be maintained near or below a desired threshold while maximizing energy savings. In particular, DCV at 800 ppm achieves minimum energy cost with transmission risk, while the novel TCV strategy at 0.05 per infector·h forgoes some of the energy savings to achieve further reduction in observed transmission rate. Note that the specific setpoints of these two strategies could be adjusted up or down to further tune the tradeoff. Finally, combining TCV with in-room far UV can achieve the same average and lower spread of transmission rate as the conservative baseline schedule with up to a tenfold decrease in energy cost.

Overall, these results illustrate that advanced control strategies and alternative sources of EOA can be employed to provide similar or better expected transmission rate while significantly reducing energy costs compared to constantly operating at high ventilation rates. We see that the TCV strategies deliver Pareto-optimal performance, which demonstrates that the pseudo-steady transmission model is sufficiently accurate to achieve its control objectives while remaining mathematically simple enough to integrate into existing HVAC control logic. Such TCV systems could interface with other sources of EOA, such as filtration and UV disinfection, to simultaneously control transmission rates and minimize energy consumption by prioritizing lower energy sources.

4. Conclusions

4.1. Summary

Our framework successfully combines data-streams from sensors with accurate physical models of aerosol physics and disease transmission to predict transmission rates in real-life, as-operated indoor spaces. Such an approach can be used both for real-time transmission control and future building design when considering indoor air quality. We have demonstrated the possibility of transmission-controlled ventilation by implementing our models in HVAC control logic, which maintains air quality at a safe level while optimally minimizing energy usage. Our simple formulas provide an easy-to-use design framework for building designers and engineers when considering the trade-off between energy efficiency and indoor air quality for installing various clean air delivery mechanisms in current and future buildings.

Our results can also inform public health guidance, using data from real buildings. We have validated the use of the simple safety guideline, Eq. (2), to limit infection risk in different classes of indoor spaces, rather than strict occupancy limits [9]. We have shown that the underlying pseudo-steady approximation is consistent with full, dynamical simulations, and whenever small discrepancies arise, the guideline always provides a more conservative estimate of the risk. For normal occupancy in the monitored spaces, we also predict that short-range transmission via respiratory flows can be neglected (compared to the long-range airborne transmission) without imposing physical distance limits.

CO_2 measurements play a central role in the analysis. Time-varying occupancy and ventilation rates are critical parameters in the models for transmission rate. When rooms are mechanically ventilated with set rates from the BMS, CO_2 measurements can be used to accurately estimate occupancy with complete anonymity to the occupants. When ventilation rates are unknown, such as for naturally ventilated spaces, CO_2 measurements can be used to estimate both occupancy and ventilation rates, albeit with larger uncertainty. Importantly, we demonstrated how CO_2 is not a direct proxy for transmission risk due to varying sources of EOA. However, with appropriate knowledge of the EOA sources, CO_2 can be used in conjunction with our models to accurately estimate transmission risk in diverse indoor spaces.

Controlling disease transmission must also be considered within the context of broader societal needs, such as minimizing energy usage, pollution, and carbon emissions. Our framework is able to quantify and optimize these tradeoffs, as the various sources of EOA are all incorporated, including their different energy requirements. We demonstrate how this modeling can be used to design optimal control protocols which control for certain transmission risk setpoints while also minimizing energy requirements by prioritizing low-energy EOA sources. Enabling real-time control of infection risk, prioritized against energy consumption, is a critical first step in the paradigm shift toward more healthy, energy efficient buildings [12].

4.2. Future work

To put these ideas into practice, there is more work to be done. First, additional validation is warranted for the proposed occupancy-estimation procedure. To achieve wide real-world adoption, any such strategy needs have simple deployment (i.e., be largely plug-and-play) while delivering sufficient accuracy. Approaches derived from physics-based models meet this first requirement because they do not require training data containing actual occupancy counts [36]. However, they do bring additional uncertainty in the physiological parameters they depend upon. Our proposed approach to regularize against assumed *peak* occupancy helps to resolve much of this uncertainty, but more extensive testing and comparison against other occupant-counting technologies would confirm whether accuracy requirements are satisfied.

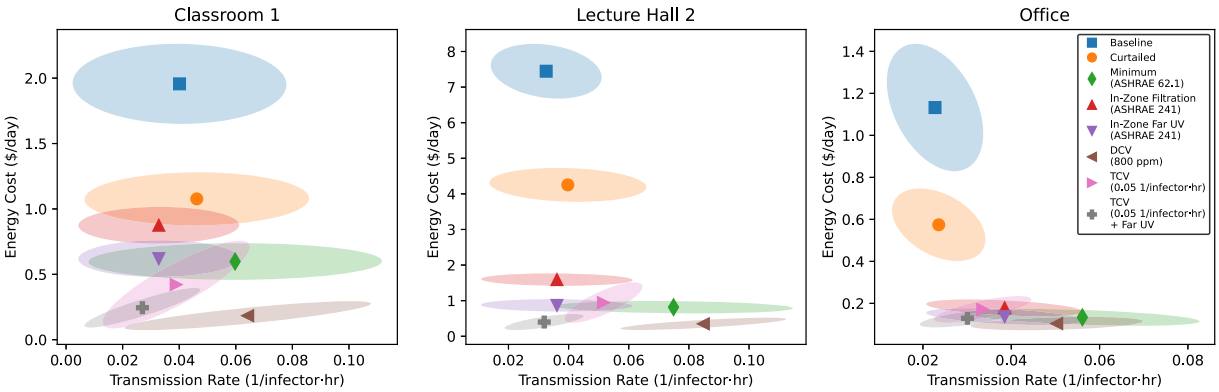

Fig. 6. Summary of energy versus transmission rate tradeoffs for hypothetical ventilation scenarios. Points and shaded regions show means and joint standard deviations for daily values within the study period. (For interpretation of the references to color in this figure legend, the reader is referred to the web version of this article.)

Second, although the well-mixed pseudo-steady model holds in many spaces, there will likely be zones where it is not a good approximation, in particular, rooms where free airflow is obstructed or where displacement ventilation is used [34]. To identify these cases, a quick verification procedure should be developed, e.g., using CO_2 (or other tracer gas) and multiple sensors placed throughout the room to quantify the degree of mixing. Situations where short-range transmission may be significant also need to be recognizable so that other precautions can be taken, as the HVAC system is largely unable to mitigate this transmission route.

Third, the strategies proposed in this paper need to be reconciled against relevant standards. The recent ASHRAE 241 [25] is a good starting point, and the ideas here are largely compatible. (Indeed, the safety guideline in (2) can be rearranged to give a requirement that $\lambda_{\mathrm{EOA}} V / N_s$ is greater than some minimum value, which is precisely what the standard requires.) However, adherence to the standard is somewhat inflexible, with EOA requirements being set based on *maximum* occupancy limits. Thus, in a space like Classroom 1 where the occupancy is above 30 for 3 h per week and almost always below 15 otherwise, operating in the standard's infection risk management mode (IRMM) would require 30 occupants worth of EOA delivery during *all* occupied hours. The practical effect is that targeted strategies like DCV and even TCV would need to be disabled, leading to unnecessary energy use with little (if any) reduction in infection risk. We hope that future versions of the standard will permit the use of dynamic EOA requirements based on real-time occupancy counts, analogous to how ASHRAE 62.1 [14] permits the use of DCV to deliver occupancy-dependent outdoor airflow.

Finally, more guidance needs to be given to building managers and other stakeholders to help them decide when and at what intensity to apply infection-control measures. Although the formulas in this paper are mathematically straightforward, their application requires a threshold to be chosen, which ultimately depends on individual risk tolerance. ASHRAE 241 makes further simplifications by effectively choosing a standard threshold for each type of space, but then the choice is ultimately reduced to the binary of operating in IRMM or not. To better contextualize this decision, the possible actions should be tied to more tangible outcomes associated with occupant health. Both for infection risk and IAQ in general, it is possible to quantify the effect on occupant productivity, often showing that mitigation strategies clearly reduce total cost even if energy consumption is slightly increased [67]. By re-framing the discussion in this way, the ideas proposed here and in other works can be viewed as actively beneficial, leading to buildings that are both sustainable and healthy.

CRediT authorship contribution statement

Michael J. Risbeck: Writing – original draft, Software, Methodology, Investigation, Conceptualization. **Alexander E. Cohen:** Writing – original draft, Methodology, Investigation, Conceptualization. **Jonathan D. Douglas:** Writing – review & editing, Methodology, Conceptualization. **Zhanhong Jiang:** Writing – review & editing, Resources. **Carlo Fanone:** Writing – review & editing, Resources. **Karen Bowes:** Writing – review & editing, Resources. **Jim Doughty:** Writing – review & editing, Resources. **Martin Turnbull:** Writing – review & editing, Resources. **Louis DiBerardinis:** Writing – review & editing, Resources. **Young M. Lee:** Writing – original draft, Conceptualization. **Martin Z. Bazant:** Writing – original draft, Methodology, Conceptualization.

Declaration of competing interest

The authors declare that they have no known competing financial interests or personal relationships that could have appeared to influence the work reported in this paper.

Data availability

The data is available on Github through a link provided in the manuscript.

Acknowledgments

A.E.C. was supported by the Department of Defense (DoD) through the National Defense Science and Engineering Graduate (NDSEG) Fellowship Program. Partial funding for this study was provided by Johnson Controls, United States of America, and portions of the research are subject to patents pending.

Appendix A. Supplementary data

Supplementary material related to this article can be found online at https://doi.org/10.1016/j.buildenv.2023.110893.

References

[1] A. Pak, et al., Economic consequences of the COVID-19 outbreak: The need for epidemic preparedness, Front. Public Health 8 (2020) 241.
[2] N. Van Doremalen, et al., Aerosol and surface stability of SARS-CoV-2 as compared with SARS-CoV-1, N. Engl. J. Med. 382 (16) (2020) 1564–1567.
[3] L. Morawska, D.K. Milton, It is time to address airborne transmission of Coronavirus disease 2019 (COVID-19), Clin. Infect. Dis. 71 (9) (2020) 2311–2313.
[4] L. Morawska, et al., COVID-19 and airborne transmission: Science rejected, lives lost. Can society do better? Clin. Infect. Dis. (2023).
[5] J.D. Sachs, et al., The lancet commission on lessons for the future from the COVID-19 pandemic, Lancet 400 (10359) (2022) 1224–1280.
[6] X. Zhang, et al., Monitoring SARS-CoV-2 in air and on surfaces and estimating infection risk in buildings and buses on a university campus, J. Exposure Sci. Environ. Epidemiol. 32 (5) (2022) 751–758.

[7] P.Y. Chia, et al., Detection of air and surface contamination by SARS-CoV-2 in hospital rooms of infected patients, Nat. Commun. 11 (1) (2020) 2800.
[8] K. Nissen, et al., Long-distance airborne dispersal of SARS-CoV-2 in COVID-19 wards, Sci. Rep. 10 (1) (2020) 1–9.
[9] M.Z. Bazant, J.W. Bush, A guideline to limit indoor airborne transmission of COVID-19, Proc. Natl. Acad. Sci. 118 (17) (2021) e2018995118.
[10] B. Blocken, et al., Ventilation and air cleaning to limit aerosol particle concentrations in a gym during the COVID-19 pandemic, Build. Environ. 193 (2021) 107659.
[11] W.G. Lindsley, et al., Efficacy of portable air cleaners and masking for reducing indoor exposure to simulated exhaled SARS-CoV-2 aerosols—-United States, 2021, Morb. Mortal. Wkly. Rep. 70 (27) (2021) 972.
[12] L. Morawska, et al., A paradigm shift to combat indoor respiratory infection, Science 372 (6543) (2021) 689–691.
[13] L. Morawska, G.B. Marks, J. Monty, Healthy indoor air is our fundamental need: The time to act is now, Med. J. Aust. 217 (11) (2022) 578–581.
[14] ASHRAE, Ventilation for acceptable indoor air quality, ANSI/ASHRAE/IES Standard 62.1-2019, 2019.
[15] W.F. Wells, Airborne Contagion and Air Hygiene: An Ecological Study of Droplet Infections, Harvard University Press, 1955.
[16] E. Riley, G. Murphy, R. Riley, Airborne spread of measles in a suburban elementary school, Am. J. Epidemiol. 107 (5) (1978) 421–432.
[17] C. Beggs, C. Noakes, P. Sleigh, L. Fletcher, K. Siddiqi, The transmission of tuberculosis in confined spaces: An analytical review of alternative epidemiological models, Int. J. Tubercul. Lung Dis. 7 (11) (2003) 1015–1026.
[18] M. Nicas, W.W. Nazaroff, A. Hubbard, Toward understanding the risk of secondary airborne infection: Emission of respirable pathogens, J. Occup. Environ. Hyg. 2 (3) (2005) 143–154.
[19] G. Buonanno, L. Morawska, L. Stabile, Quantitative assessment of the risk of airborne transmission of SARS-CoV-2 infection: Prospective and retrospective applications, Environ. Int. 145 (2020) 106112.
[20] B.L. Augenbraun, et al., Assessment and mitigation of aerosol airborne SARS-CoV-2 transmission in laboratory and office environments, J. Occup. Environ. Hyg. 17 (10) (2020) 447–456.
[21] S.L. Miller, et al., Transmission of SARS-CoV-2 by inhalation of respiratory aerosol in the skagit valley chorale superspreading event, Indoor Air 31 (2) (2021) 314–323.
[22] C.C. Wang, et al., Airborne transmission of respiratory viruses, Science 373 (6558) (2021).
[23] A. Foster, M. Kinzel, Estimating COVID-19 exposure in a classroom setting: A comparison between mathematical and numerical models, Phys. Fluids 33 (2) (2021) 021904.
[24] ASHRAE Epidemic Task Force, Building Readiness, Tech. Rep., 2022, Accessed: 07 Nov 2022.
[25] ASHRAE, Control of Infectious Aerosols, ASHRAE Standard 241–2023, 2023.
[26] S. Rudnick, D.K. Milton, Risk of indoor airborne infection transmission estimated from carbon dioxide concentration, Indoor Air 13 (3) (2003) 237–245.
[27] M.Z. Bazant, et al., Monitoring carbon dioxide to quantify the risk of indoor airborne transmission of COVID-19, Flow 1 (2021) E10.
[28] Z. Peng, J.L. Jimenez, Exhaled CO2 as a COVID-19 infection risk proxy for different indoor environments and activities, Environ. Sci. Technol. Lett. 8 (5) (2021) 392–397.
[29] J. Raymenants, et al., Indoor air surveillance and factors associated with respiratory pathogen detection in community settings in Belgium, Nature Commun. 14 (1) (2023) 1332.
[30] US Environmental Protection Agency, Exposure Factors Handbook, National Center for Environmental Assessment, Washington, DC, 2011.
[31] F. Yang, A.A. Pahlavan, S. Mendez, M. Abkarian, H.A. Stone, Towards improved social distancing guidelines: Space and time dependence of virus transmission from speech-driven aerosol transport between two individuals, Phys. Rev. Fluids 5 (12) (2020) 122501.
[32] M. Abkarian, S. Mendez, N. Xue, F. Yang, H.A. Stone, Speech can produce jet-like transport relevant to asymptomatic spreading of virus, Proc. Natl. Acad. Sci. 117 (41) (2020) 25237–25245.
[33] L. Bourouiba, E. Dehandschoewercker, J.W. Bush, Violent expiratory events: On coughing and sneezing, J. Fluid Mech. 745 (2014) 537–563.
[34] C. Zhang, et al., The source control effect of personal protection equipment and physical barrier on short-range airborne transmission, Build. Environ. 211 (2022) 108751.
[35] A. Franco, F. Leccese, Measurement of CO2 concentration for occupancy estimation in educational buildings with energy efficiency purposes, J. Build. Eng. 32 (2020) 101714.
[36] M. Zuraimi, et al., Predicting occupancy counts using physical and statistical CO2-based modeling methodologies, Build. Environ. 123 (2017) 517–528.
[37] D. Calì, P. Matthes, K. Huchtemann, R. Streblow, D. Müller, CO2 based occupancy detection algorithm: Experimental analysis and validation for office and residential buildings, Build. Environ. 86 (2015) 39–49.
[38] H. Rahman, H. Han, Bayesian estimation of occupancy distribution in a multi-room office building based on CO2 concentrations, Build. Simul. 11 (3) (2018) 575–583.
[39] S. Wolf, D. Calı, J. Krogstie, H. Madsen, Carbon dioxide-based occupancy estimation using stochastic differential equations, Appl. Energy 236 (2019) 32–41.
[40] S. Wang, X. Jin, CO2-based occupancy detection for on-line outdoor air flow control, Indoor Built Environ. 7 (3) (1998) 165–181.
[41] S. Wang, J. Burnett, H. Chong, Experimental validation of CO2-based occupancy detection for demand-controlled ventilation, Indoor Built Environ. 8 (6) (1999) 377–391.
[42] C. Jiang, M.K. Masood, Y.C. Soh, H. Li, Indoor occupancy estimation from carbon dioxide concentration, Energy Build. 131 (2016) 132–141.
[43] L.M. Candanedo, V. Feldheim, Accurate occupancy detection of an office room from light, temperature, humidity and CO2 measurements using statistical learning models, Energy Build. 112 (2016) 28–39.
[44] A. Szczurek, M. Maciejewska, T. Pietrucha, Occupancy determination based on time series of CO2 concentration, temperature and relative humidity, Energy Build. 147 (2017) 142–154.
[45] B. Dong, et al., An information technology enabled sustainability test-bed (ITEST) for occupancy detection through an environmental sensing network, Energy Build. 42 (7) (2010) 1038–1046.
[46] S.H. Ryu, H.J. Moon, Development of an occupancy prediction model using indoor environmental data based on machine learning techniques, Build. Environ. 107 (2016) 1–9.
[47] T.H. Pedersen, K.U. Nielsen, S. Petersen, Method for room occupancy detection based on trajectory of indoor climate sensor data, Build. Environ. 115 (2017) 147–156.
[48] ASHRAE, Energy Standard for Buildings Except Low-Rise Residential Buildings, ANSI/ASHRAE/IES Standard 90.1-2019, 2019.
[49] H. Tan, A. Dexter, Estimating airflow rates in air-handling units from actuator control signals, Build. Environ. 41 (10) (2006) 1291–1298.
[50] Y. Choi, S. Yoon, Virtual sensor-assisted in situ sensor calibration in operational HVAC systems, Build. Environ. 181 (2020) 107079.
[51] G. Han, J. Srebric, E. Enache-Pommer, Different modeling strategies of infiltration rates for an office building to improve accuracy of building energy simulations, Energy Build. 86 (2015) 288–295.
[52] L.C. Ng, A.K. Persily, S.J. Emmerich, Improving infiltration modeling in commercial building energy models, Energy Build. 88 (2015) 316–323.
[53] L.C. Ng, et al., Estimating real-time infiltration for use in residential ventilation control, Indoor Built Environ. 29 (4) (2020) 508–526.
[54] L.C. Ng, J. Wen, Estimating building airflow using CO2 measurements from a distributed sensor network, HVAC&R Res. 17 (3) (2011) 344–365.
[55] S. Park, P. Choi, D. Song, J. Koo, Estimation of the real-time infiltration rate using a low carbon dioxide concentration, J. Build. Eng. 42 (2021) 102835.
[56] D.R. Dunn, Monthly Energy Review, April 2022, Section 2, Tech. Rep. DOE/EIA-0035(2022/4), US Energy Information Administration, 2022.
[57] B. Abboushi, et al., Energy Implications of Using Upper Room Germicidal Ultraviolet Radiation and HVAC Strategies to Combat SARS-CoV-2, Tech. Rep., Oak Ridge National Lab.(ORNL), Oak Ridge, TN (United States), 2022.
[58] A.R. Escombe, et al., Upper-room ultraviolet light and negative air ionization to prevent tuberculosis transmission, PLoS Med. 6 (3) (2009) e1000043.
[59] M. First, S.N. Rudnick, K.F. Banahan, R.L. Vincent, P.W. Brickner, Fundamental factors affecting upper-room ultraviolet germicidal irradiation—part I. Experimental, J. Occup. Environ. Hyg. 4 (5) (2007) 321–331.
[60] S.N. Rudnick, M.W. First, Fundamental factors affecting upper-room ultraviolet germicidal irradiation—Part II. Predicting effectiveness, J. Occup. Environ. Hyg. 4 (5) (2007) 352–362.
[61] M. Buonanno, D. Welch, I. Shuryak, D.J. Brenner, Far-UVC light (222 nm) efficiently and safely inactivates airborne human Coronaviruses, Sci. Rep. 10 (1) (2020) 1–8.
[62] E. Eadie, et al., Far-UVC (222 nm) efficiently inactivates an airborne pathogen in a room-sized chamber, Sci. Rep. 12 (1) (2022) 1–9.
[63] US Energy Information Administration, Commercial buildings energy consumption survey, 2018, Accessed 31 July 2023.
[64] R.K. Bhagat, M.D. Wykes, S.B. Dalziel, P. Linden, Effects of ventilation on the indoor spread of COVID-19, J. Fluid Mech. 903 (2020) F1.
[65] M.J. Risbeck, et al., Quantifying the tradeoff between energy consumption and the risk of airborne disease transmission for building HVAC systems, Sci. Technol. Built Environ. 28 (2022) 240–254.
[66] M.J. Risbeck, et al., Modeling and multiobjective optimization of indoor airborne disease transmission risk and associated energy consumption for building HVAC systems, Energy Build. 253 (2021) 111497.
[67] P. MacNaughton, et al., Economic, environmental and health implications of enhanced ventilation in office buildings, Int. J. Environ. Res. Public Health 12 (11) (2015) 14709–14722.